Scalings of the plasma transportation in the long helical mirror

A.V. Sudnikov[1], I.A. Ivanov[1], A.A. Inzhevatkina[1], M.V. Larichkin[2], K.A. Lomov[2], V.V. Postupaev[1], M.S. Tolkachev[2], V.O. Ustyuzhanin[2]

[1] *Budker Institute of Nuclear Physics, Novosibirsk, Russia*

[2] *Novosibirsk State University, Novosibirsk, Russia*

Introduction

The creation of an open trap with the reactor-grade plasma is achievable with the specialized magnetic sections for the suppression of the particle and energy losses along the magnetic field. The project of the next generation of the open trap GDMT includes the central gas-dynamic cell and improved axial confinement [1]. Basic method of suppression of the axial flux is the multiple-mirror confinement [2].

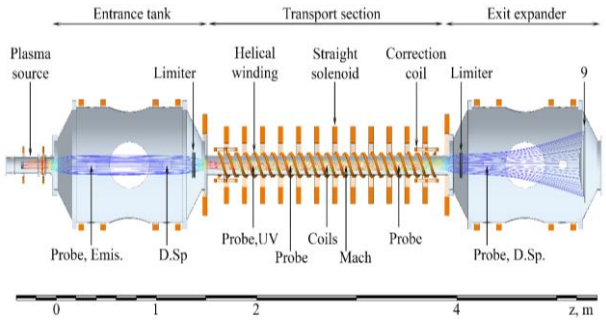

Fig. 1. SMOLA device. The plasma source, the vacuum and the magnetic systems, the limiters and the diagnostics are shown. Calculated field lines start on the edge of the cathode.

The idea of the helical mirror [3] considers a rotating plasma flow through a linear static magnetic system with helical corrugation. Periodical variations of the magnetic field moving upstream in the plasma's frame of reference transfer momentum to the trapped particles and lead to the plasma pumping towards the central trap. The helical mirror should have two improvements over the classical multiple mirrors: the exponential law of the flow suppression with the length and the radial pinch of the ions that can counteract the radial diffusion [4, 5].

Flux suppression was shown in the first experimental campaign of the «SMOLA» helical mirror [6], integral suppression ratio of 2–2.5 was achieved [7]. An increased suppression at high corrugation ratio and plasma rotation velocity was demonstrated [8]. Here we report the latest experimental results on the plasma flows in the helical mirror in a broad range of the plasma densities at high rotation velocity and high corrugation ratio.

Experimental setup and parameters

Layout of the SMOLA helical mirror [6] is shown on the Fig. 1. This experimental campaign was focused on the axial plasma fluxes in the transport section. In the discussed experiments the mirrors were asymmetric with mirror ratios $R \approx 8$ to the plasma source and $R \approx 3$ to the transport section. The guiding magnetic field in the transport section was B_z = 40–100 mT.

This section has $N = 12$ helical periods. The ratio of the maximal and the minimal magnetic field along the field line within the transport section averaged over the plasma cross-section was R_{mean} = 1–1.7. The trapped plasma density was in the range $n = (0.5–4)\cdot10^{18}$ m^{-3}, temperatures were $T_i \approx$ 4 eV and $T_e \approx$ 30 eV. These values correspond to the mean free path of an ion in the entrance tank with respect to the Coulomb scattering λ = 0.2–1.6 m. The density in the transport section is by the factor 1.5–2 lower, thus giving the ratio of the mean free path to the period of the corrugation $\lambda/h \sim 1–N$. Rotation velocity was $\omega = (1–1.2)\cdot10^6$ s^{-1} in the entrance tank and $\omega = (0.6–0.8)\cdot10^6$ s^{-1} at the exit.

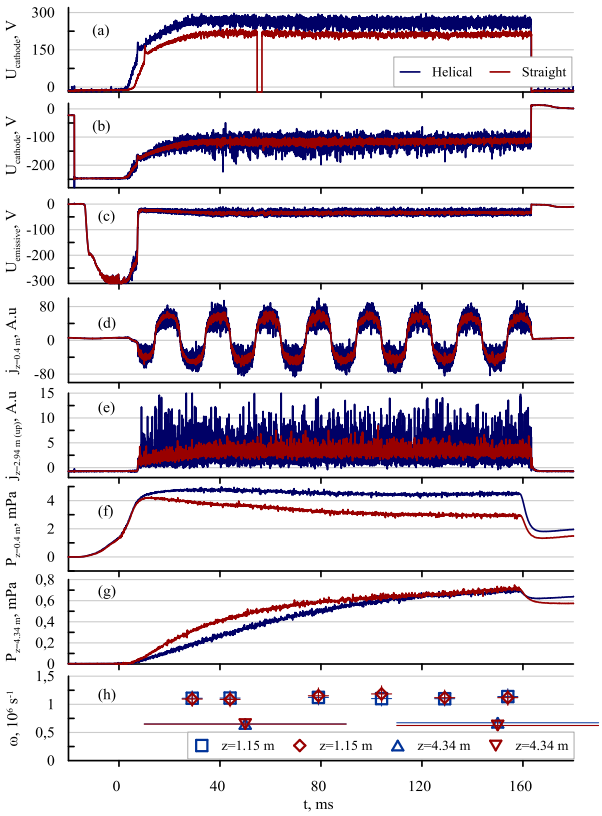

Fig. 2. Typical waveforms in the discharges with straight (red) and helical (blue) magnetic configurations: (a) discharge current; (b) voltage in the plasma source; (c) potential of the emissive probe at z=0.4 m; (d) current of the double probe at z=0.4 m (I-V curve); (e) current of the upstream side of the Mach probe (ion saturation); (f, g) neutral hydrogen pressure at z=0.4 m and z=4.34 m, (h) rotation velocity at z=1.15 m and z=4.34 m.

The main diagnostic for the flux densities was the set of the double, emissive and Mach probes distributed over the length of the device. The Mach probe was oriented normally to the guiding magnetic field, so the upstream and downstream sides collect only the ions with $v_z > 0$ and $v_z < 0$, correspondingly. The Doppler spectrometers and the Mirnov coils were used to measure plasma rotation [9]. Typical experimental waveforms are shown on Fig. 2. Plasma parameters were stable during the experiments. Average values on the flattop of the discharge were used to build up the radial profiles of the plasma parameters.

Results and discussion

One can observe the rise of the plasma density with the activation of the helical field (Fig.3). The amplitude of the plasma flux and the width of the plasma stream at the exit from the transport section decrease significantly. Another notable effect is the significant rise of the flux density on the downstream side of the Mach probe. Near the axis, this flux density becomes higher than the flux density going in the normal direction.

The dependencies of the integrated fluxes on the relative amplitude of the helical component of the magnetic field are shown on Fig. 5. The clearest evidence of the helical mirror effect is 1.6-fold rise in the number of the particles confined between the simple mirror and the helical one (Fig. 5 a). It agrees well with the significant drop in the particle flux at the exit from the transport section (Fig. 5 c). At the high corrugation ratio (R_{mean} = 1.7) this integral flux drops below the detectable level. More detailed information on the axial flux was obtained by the Mach probe (Fig. 5 b). The integral flux from the plasma source towards the exit gradually decreases, while the return flux increases by the factor of 1.5. At highest achievable corrugation ratio the difference between the outcoming and return fluxes becomes lower than the confidence interval.

The dependence of the integral fluxes on the plasma density (Fig. 4) was measured at guide magnetic field B_z = 70mT and mean corrugation ratio R_{mean} = 1.35. All fluxes, including the flux on the downstream side of the Mach probe, scale linearly with the gas feeding of the plasma source. No significant difference in the densities of the forward and return fluxes normalized by the density in the entrance was observed. Return flux is observed even at low classical collisionality.

If the density inside the entrance tank exceeds $n \sim 10^{18}$ m^{-3} the losses are gas dynamic. They are balanced with the feed from the plasma source and the return flux from the transport section. Direct calculation of the effective mirror ratio R_{eff} is obstruct because the difference between F_{feed} and gas dynamic losses to the simple mirror is close to zero. The lower estimate may be evaluated, giving $R_{eff} > 10$ at R_{mean} = 1.7.

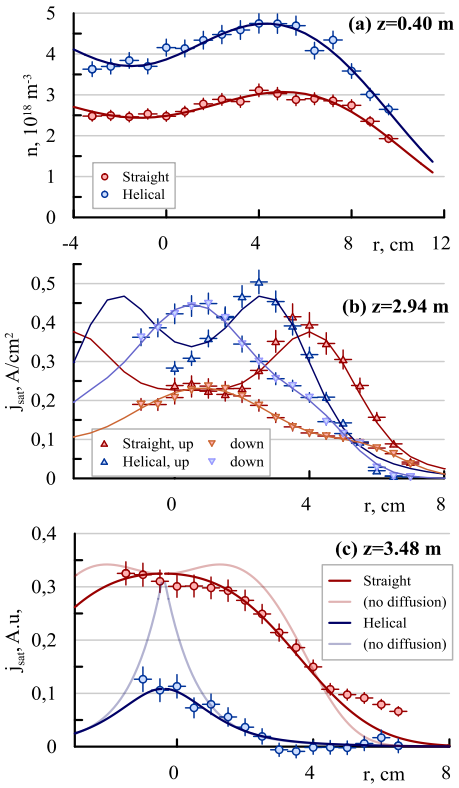

Fig. 3. Sample radial profiles at R_{mean} = 1.55. (a) density in the entrance tank (fitted); (b) flux in the middle of the transport section on the upstream and downstream sides of the Mach probe (fitted); (c) flux at the exit of the transport section (modelled).

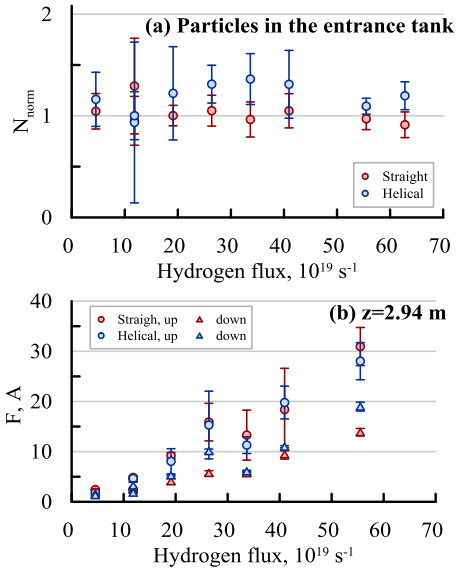

Fig. 4. Dependence of the particle number and integral flux on the gas feeding of the plasma source.

The return flux with the local density on the axis excessing the density of the flux in the forward direction was observed directly. Its occurrence takes place jointly with the reduction of the width of the forward flux. Both of these facts stand in the qualitative agreement with the theoretical model. This return flux should consist of the trapped particles and therefore have the mean velocity comparable to the axial velocity of the multiple mirror movement. Such flux by itself can be a source of the energy for the microinstabilities, which lead to the anomalous scattering. Presence of the anomalous scattering is required to obtain high efficiency of the multiple mirror confinement if the mean free path with respect to Coulomb scattering is higher than the period of the magnetic corrugation. Linear dependence of the experimentally measured particle fluxes on the plasma density and higher level of the noise in the probe data in the helical configuration may be the indirect evidences of this process, but the question of the microinstability level requires further investigations.

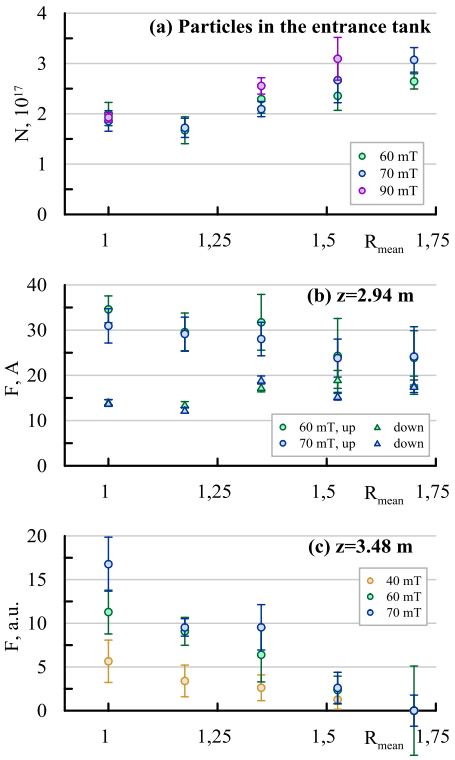

Fig. 5. Dependence of the particle number and integral flux on the corrugation ratio.

The density profiles at the exit were modeled. Real experimental density at the entrance of the transport section, corrugation ratio and angular velocity were used for calculation. One can observe good agreement of the calculated profiles and the experimental ones (Fig. 3c).

Acknowledgements

This work was supported by Russian Science Foundation (project No. 18-72-10080). Parts of the study related to the particle balance were supported by the grant of the President of Russian Federation SP-1242.2021.2.

[1] A. BEKLEMISHEV, et al., *Fusion Sci. Technol.* **63** (1T), 46 (2013).
[2] V. V. POSTUPAEV, et al., Nuclear Fusion **57**, 036012 (2017).
[3] A. BEKLEMISHEV, Fusion Sci. Technol. **63** (1T), 355 (2013).
[4] A. BEKLEMISHEV, AIP Conference Proceedings **1771**, 040006 (2016).
[5] I. CHERNOSHTANOV, D. AYUPOV, Phys. of Plasmas **28**, 032502 (2021).
[6] A. V. SUDNIKOV, et al., Fusion Eng. Design. **122**, 85 (2017).
[7] A. V. SUDNIKOV, Plasma and Fusion Research, **14**, 2402023 (2019).
[8] A. V. SUDNIKOV, et al., J. Plasma Phys. **86** (5), 905860515 (2020).
[9] A. A. INZHEVATKINA, et al, Plasma Phys. Rep., In press (2021).